AIChE

A Multi-Scale Theoretical Model for Gas–Liquid Interface Mass Transfer Based on the Wide Spectrum Eddy Contact Concept

Luchang Han, Hean Luo, Yuejin Liu, Kuiyi You, and Pingle Liu
College of Chemical Engineering, Xiangtan University, Hunan 411105, P.R. China

DOI 10.1002/aic.12327
Published online July 13, 2010 in Wiley Online Library (wileyonlinelibrary.com).

On the basis of the wide spectrum eddy contact concept and the isotropic turbulence theory, a multi-scale theoretical model for the prediction of liquid-side mass transfer coefficient in gas–liquid system was developed. The model was derived from an unsteady-state convection and diffusion equation and considered the contributions of eddies with different sizes to the overall mass transfer coefficient. The proper contact time distribution at the surface is need to be determined to obtain satisfactory results with this model. Moreover, a simplified model was also proposed based on the assumption of steady-state mass transfer mechanism for single eddy. The results predicted by this model showed a very good agreement with the available experimental data in a comparatively wide range of turbulence intensities. © 2010 American Institute of Chemical Engineers *AIChE J,* 57: 886–896, 2011
Keywords: mass transfer, eddy contact, interface, gas–liquid, breakup

Introduction

Gas–liquid mass transfer process widely exists in many industries such as chemical, food, medicine, and petroleum. The mechanism of interface mass transfer is the basis of understanding these mass transfer processes, to be capable of predicting mass transfer rate and designing proper equipment for the processes. Since the two-film theory[1] was proposed in 1924, the theoretical and experimental research for mass transfer has been developed at the same time. Many theories and models, such as penetration theory,[2] surface renewal theory,[3] and their improved models,[4–8] eddy concept model,[9–12] and statistics theory,[13] have been proposed. A large number of experiential correlations with regard to several key parameters, for example, per unit volume power and superficial gas velocity, have been presented.[14–16] These correlations play the role of scale-up and optimization design for many industrial plants, although they usually can't be extended to other operation conditions arbitrarily. Experimental studies also promote the development of mass transfer theories at the same time.

In the previous literature, more attention has been paid to the mass transfer models based on the penetration or surface renewal theory, since they only need to determine an unknown parameter, for instance exposure (or contact) time or surface renewal rate. Several estimation methods for these parameters have been proposed by different investigators. Two methods are discussed frequently among these estimation methods. The first is based on the isotropic turbulence theory and takes the ratio of Kolmogorov scale to turbulent fluctuation velocity as the exposure time of eddies on the surface, as known as "eddy" models. Most "eddy" models from this method have a similar form:

$$k_L = c_0\sqrt{D}(\varepsilon/\nu)^{1/4} \tag{1}$$

where c_0 is a constant, different authors have offered various values such as 0.301,[17] 0.4,[10] 0.531,[15] 0.592,[18] and 1.13.[19] The second defines the exposure time as the ratio of bubble diameter to bubble slip velocity, known as "slip penetration"

Correspondence concerning this article should be addressed to H. Luo at hluo@xtu.edu.cn.

model, in which the mass transfer coefficient is an explicit function of the diameter of bubble. The main difference between the two methods mentioned above is in the effect of liquid turbulence intensity on the mass transfer coefficient. The "eddy" models show an increase of k_L with increasing turbulence intensity, while the "slip penetration" model predicts a dependence of k_L on the bubble diameter but turbulence intensity.[15,20] In the case of surface contaminated by surfactants, contrary to the "eddy" models, the "slip penetration" model predicts a decrease of k_L with increasing turbulence intensity. Linek et al.[15] have pointed out that because bubble surface becomes rigid at higher turbulence intensities, and k_L from a rigid surface is smaller than that from a mobile surface at lower turbulence intensities.[15]

As well known, the one-dimensional unsteady-state diffusion equation is very easy to be manipulated and even got an analytical solution, because there is no need to know the fluid element velocity close to the surface. However, it should be noted that the assumption that the molecular diffusion governs the mass transfer process may not be appropriate as the contribution of convection to mass transfer becomes predominant with increase of turbulence intensity, although it has been adopted by the classical penetration or surface renewal models, two-film model,[1] penetration model,[2] surface renewal model,[3] and film penetration model.[5] If the convection close to the surface is considered, an unsteady-state convection and diffusion equation has to be worked out, where the velocity distribution must be known in advance. Because obtaining an analytical solution for a three-dimensional equation is still very difficult and even hardly possible at present, certain simplifications and assumptions must be made. For example, the eddy concept models assumed a two-dimensional steady-state mass transfer mechanism containing convection and diffusion,[9–11] and the recent more complex surface renewal-stretch model from the penetration theory further considered a one-dimensional unsteady-state mechanism of convection and diffusion normal to the surface.[8]

The main difference between the eddy concept models and the classical penetration (or surface renewal) models is that the former assumes the eddy velocity close to the surface can be accurately predicted by using a function based on the turbulence theory, and the mass transfer is steady-state and mainly controlled by certain scales of eddies, for example, large-scale containing-energy eddies (viz. large-eddy model[9]) or small-scale viscosity eddies (viz. small-eddy model[10]), while the latter usually assumes the mass transfer is unsteady-state and takes exposure time or surface renewal rate to account for the difference among fluid elements.

The eddy concept models relating their parameters with turbulence micro-structure are the further development of mass transfer theory. In these models, the large-eddy model needs to determine the integral scale and the turbulence intensity of bulk fluid, but these parameters are usually unclear because the turbulence is anisotropic in the energy containing range, unlike in the inertia subrange or the dissipation range. This makes the large-eddy model not easy to be applied. In a sense, the small-eddy model seems more convenient and advanced due to its considering the influence of eddies with different sizes in the dissipation range on the mass transfer coefficient and establishes a theoretic relationship between the turbulence intensity and the liquid-side mass transfer coefficient, k_L. The small-eddy model has been supported by some experimental results at high turbulence intensities. However, there are still some controversies about which scale of eddies (large-scale or small-scale or else) governs the mass transfer process on the surface.[10,21–23]

On the basis of the single eddy concept, Luk and Lee[11] assumed the fluid in liquid side of surface comprising a series of isotropic turbulent eddies and proposed a single-eddy model. Although the whole mass transfer of eddies is unsteady-state, the single-eddy mass transfer may be regarded as steady state. Furthermore, they assumed that the eddy velocity close to the surface could be predicted by a sinusoidal distribution function.[11] If the amplitude of velocity is known, the mass transfer coefficient of each eddy can be obtained. According to the single-eddy model, the average mass transfer coefficient of each eddy has a direct relationship with the eddy length scale and the velocity amplitude of eddy. Luk and Lee haven't given the theoretical estimation method for these parameters, but performed a series of experimental measurements on gas–liquid surface to obtain their values. Unfortunately, the experimental measurement has been greatly limited by technique and is thus troublesome to predict the mass transfer coefficient of practical fluids.

This work aims to develop a novel theoretical model for estimating the mass transfer coefficient based on a wide spectrum eddy contact concept. Unlike previous work of the eddy concept models, the present work will start from an unsteady-state convection and diffusion mechanism and consider the contributions of eddies with different sizes to mass transfer coefficient in a wider range of wave spectrum.

Theoretical Development

In gas–liquid systems, mass transfer processes close to interface are very complex. Hence, this work needs to make the simplifications as follows.

1. Following Luk and Lee,[11] the fluid in liquid side of surface is considered to comprise a series of eddies with different sizes and the turbulent fluctuation of eddies close to surface can be expressed by a sinusoidal velocity distribution function.

2. The liquid turbulence is usually supposed to be isotropic. This assumption is fairly acceptable although actual turbulence isn't completely isotropic. This is because theoretical considerations and experimental evidence have shown that the fine-scale structure of most actual anisotropic turbulent flows is locally nearly isotropic.[24,25] Many features of isotropic turbulence may thus be applied to phenomena in actual turbulence those are determined mainly by the fine-scale structure.[24]

3. In the case of surface occurring turbulent flows, fluid elements or eddies may be in the situation of frequent deformation and elongate, the convection of eddies close to surface may become important for the interface mass transfer. For simplicity, only the mass transfer process in the direction perpendicular to the interface is considered.

4. Since the exposure (or contact) time is usually very short, the velocity distribution in an eddy is thus assumed to be unvaried with time, whereas mass transfer may be

subjected to an unsteady state during the contact between eddy and bubble surface.

According to Luk and Lee, the velocity distribution in an eddy in the x direction may be written as

$$u = A\sin(\pi x/\lambda) \tag{2}$$

where x is the direction parallel to the surface, A is the velocity amplitude in the x direction, and λ is the length scale of eddy. Considering the two-dimensional flows close to the surface, the equation of continuity can be simplified from the mass conservation as

$$\frac{\partial u}{\partial x} + \frac{\partial v}{\partial y} = 0 \tag{3}$$

.Combining Eqs. 2 and 3, it gives

$$v = -yA\frac{\pi}{\lambda}\cos\left(\frac{\pi}{\lambda}x\right) = -yH \tag{4}$$

where y is the direction perpendicular to the surface and H is just a denotative variable of x for convenience. According to the assumptions mentioned above, the convection–diffusion equation for the solute concentration can be written as

$$\frac{\partial c}{\partial t} - yH\frac{\partial c}{\partial y} = D\frac{\partial^2 c}{\partial y^2} \tag{5}$$

Its initial and boundary conditions are:

$$c|_{t=0} = c_b\ ; \quad c|_{y=0} = c_s\ ; \quad c|_{y=\delta} = c_b \tag{6}$$

where c_b and c_s are the solute concentrations in bulk and at surface, respectively. Equation 5 is partial differential equation that can be solved by the common method of variable separation. However, if define

$$c = c(\phi) \quad \text{where} \quad \phi = yT(t) \tag{7}$$

Equation 5 becomes an ordinary differential type

$$\frac{d^2 c}{d\phi^2} + \Omega\phi\frac{dc}{d\phi} = 0 \tag{8}$$

where

$$\Omega = \frac{HT - T'}{DT^3} \tag{9}$$

Letting Ω be a constant and combing the boundary conditions given in Eqs. 6 and 8 gives

$$c = c_s + \frac{c_b - c_s}{\mathrm{erf}(\delta T(t)\sqrt{\Omega/2})}\mathrm{erf}(yT(t)\sqrt{\Omega/2}) \tag{10}$$

Obviously, only when $T(0)\to\infty$, Eq. 10 can satisfy the initial condition given in Eq. 6. On the other hand, considering Ω is a constant and $T(0)\to\infty$, Eq. 9 can give

$$T(t) = \sqrt{\frac{H}{D\Omega[1-\exp(-2Ht)]}} \tag{11}$$

Substitute Eq. 11 into Eq. 10 and obtain

$$c = c_s + \frac{c_b - c_s}{\mathrm{erf}\left(\delta\sqrt{\frac{H}{2D[1-\exp(-2Ht)]}}\right)}\mathrm{erf}\left(y\sqrt{\frac{H}{2D[1-\exp(-2Ht)]}}\right) \tag{12}$$

The mass transfer coefficient model derived from Eq. 12 will be a triple integral, which is very convoluted to be employed for practical purposes. We note that the denominator in Eq. 12 is an error function, erf(ω) (where $\omega = \delta\sqrt{\frac{H}{2D[1-\exp(-2Ht)]}}$. When taking the depth of liquid film δ as eddy size and the eddy contact time is taken as the Kolmogorov time scale, ω will be nearly always much more than 2 and erf(ω) tends to one quickly, thus we may neglect the denominator, then the triple integral can be simplified as a double type. Nevertheless, in the case of steady state, it becomes $\mathrm{erf}\left(\delta\sqrt{H/(2D)}\right)$, which is independent on the contact time and will be contained in the steady-state model. Then, Eq. 12 becomes

$$c = \begin{cases} c_s + (c_b - c_s)\mathrm{erf}\left(y\sqrt{\frac{H}{2D(1-\exp(-2Ht))}}\right) & \text{i} \\ c_s + \dfrac{c_b - c_s}{\mathrm{erf}\left(\delta\sqrt{H/(2D)}\right)}\mathrm{erf}\left(y\sqrt{H/(2D)}\right) & \text{ii} \end{cases} \tag{13}$$

where i and ii denote the unsteady-state and the steady-state mass transfer for single eddy, respectively. Substituting Eq. 13 into the following local mass transfer coefficient expression

$$k_{\mathrm{Local}} = -\frac{D}{c_s - c_b}\left.\frac{\partial c}{\partial y}\right|_{y=0} \tag{14}$$

Then

$$k_{\mathrm{Local}} = \begin{cases} \dfrac{\sqrt{2DH/\pi}}{\sqrt{1-\exp(-2Ht)}} & \text{i} \\ \dfrac{\sqrt{2DH/\pi}}{\mathrm{erf}\left(\delta\sqrt{H/(2D)}\right)} & \text{ii} \end{cases} \tag{15}$$

And the average mass transfer coefficient of single eddy, $\overline{k}_\lambda$ can be obtained by integrating with respect to x and t

$$\overline{k}_\lambda = \begin{cases} \dfrac{2}{\pi\tau_e}\sqrt{\dfrac{2DA}{\lambda}}\displaystyle\int_0^{\tau_e}\int_0^{\pi/2}\frac{\sqrt{\cos(\varphi)}}{\sqrt{1-\exp(-2A\pi\cos(\varphi)t/\lambda)}}d\varphi dt & \text{i} \\ \dfrac{2}{\pi}\sqrt{\dfrac{2DA}{\lambda}}\displaystyle\int_0^{\pi/2}\frac{\sqrt{\cos(\varphi)}}{\mathrm{erf}\left(\delta\sqrt{\dfrac{A\pi\cos(\varphi)/\lambda}{2D}}\right)}d\varphi & \text{ii} \end{cases} \tag{16}$$

where $\varphi = \pi x/\lambda$, τ_e is the exposure (or contact) time of fluid element. In order to obtain $\overline{k}_\lambda$, it needs to determine the amplitude of velocity, A in Eq. 16. Measuring the statistical distribution of A of eddies with different sizes close to the surface is very difficult at present due to the complexity of actual fluid flows. According to the suggestion given by Lamont and Scott,[10] there is a proportional relationship among A, wave number n and energy spectrum $E(n)$. Therefore, A can be expressed as

$$A \propto \sqrt{nE(n)} = c_1\sqrt{nE(n)} \tag{17}$$

where c_1 is a proportion constant, Lamont and Scott have given a value of 0.4 according to the isotropic turbulence

theory. It is worth noting that the one-dimensional form of $E(n)$ is needed since A denotes an one-dimensional velocity amplitude. Through Eq. 17, $\overline{k}_\lambda$ can be expressed as a function only depending on wave number n. Therefore, $\overline{k}_\lambda$, which was obtained only through experiment originally, can be estimated theoretically now. Obviously, it will bring great convenience, but only knowing the mass transfer coefficient of single eddy is not enough. To obtain the overall average mass transfer coefficient at the surface, it is necessary to consider the contribution of eddies with different sizes to the overall mass transfer coefficient, thus the following express can be derived

$$k_{\mathrm{L}} = \frac{\int_{n_d}^{n_u} \overline{k}_\lambda E(n) dn}{\int_{n_d}^{\mathrm{n_u}} E(n) dn} \tag{18}$$

Substituting Eq. 16 into Eq. 18 and obtain

$$k_{\mathrm{L}} = \begin{cases} \dfrac{2\sqrt{2c_1 D}}{\pi \displaystyle\int_{n_d}^{n_u} E(n) dn} \displaystyle\int_{n_d}^{\mathrm{n_u}} \int_0^{\tau_e} \int_0^{\pi/2} \dfrac{E(n)^{5/4} n^{3/4} \sqrt{\cos(\varphi)}}{\tau_e \sqrt{1 - \exp\left(-2c_1 \pi E(n)^{1/2} n^{3/2} \cos(\varphi) t\right)}} d\varphi dt dn & \text{i} \\ \dfrac{2\sqrt{2c_1 D}}{\pi \displaystyle\int_{n_d}^{\mathrm{n_u}} E(n) dn} \displaystyle\int_{n_d}^{\mathrm{n_u}} \int_0^{\pi/2} \dfrac{E(n)^{5/4} n^{3/4} \sqrt{\cos(\varphi)}}{\mathrm{erf}\left(\delta \sqrt{c_1 \pi / 2D} E(n)^{1/4} n^{3/4} \sqrt{\cos(\varphi)}\right)} d\varphi dn & \text{ii} \end{cases} \tag{19}$$

The triple integral given in Eq. 19i can be simplified into a double integral, which can greatly decrease the calculation cost

$$k_{\mathrm{L}} = \frac{2\sqrt{2D/c_1}}{\pi^2 \int_{\mathrm{n_d}}^{\mathrm{n_u}} E(n) dn} \int_{n_d}^{\mathrm{n_u}} \int_0^{\pi/2} \frac{E(n)^{3/4} n^{-3/4}}{\tau_e \sqrt{\cos(\varphi)}} \arctan h\left(\sqrt{1 - \exp(-2c_1 \pi E(n)^{1/2} n^{3/2} \cos(\varphi) \tau_e)}\right) d\varphi dn \tag{20}$$

Energy Spectrum Function

The energy spectrum function $E(n)$ must be known before solving Eq. 19. In the literature, most results of $E(n)$ focused on the inertia subrange for validating the $-5/3$ power law, whereas the available data in the other ranges were very limited. Only the following two models can be found from the literature.

Model A

Pope has proposed a three-dimensional energy spectrum function as follows[26]

$$E(n) = C\varepsilon^{2/3} n^{-5/3} \left\{ n\lambda_e \Big/ \left[(n\lambda_{\mathrm{e}})^2 + c_{\mathrm{L}} \right]^{1/2} \right\}^{5/3+p_0} \exp\left\{ -\beta \left[(n\eta)^4 + c_\eta^4 \right]^{1/4} + \beta c_\eta \right\} \tag{21}$$

where C is the Kolmogorov constant, Yeung et al. have given a value of 0.53 for the one-dimensional energy spectrum based on the isotropic turbulence theory.[27] The other constants appearing in Eq. 21 are

$$\alpha = 0.4;\ c_{\mathrm{L}} \approx 6.78;\ c_\eta \approx 0.40;\ p_0 = 2;\ \beta = 5.2. \tag{22}$$

Model B

According to Hinze,[24] the energy spectrum from Kolmogorov scale to inertia subrange can be defined as:

$$E_1(n) = (\varepsilon v^5)^{1/4} [1.61(n\eta)^{-5/3} + 2.5(n\eta)^{-1}] \exp[-2.41(n\eta)^{4/3} - 2.5(n\eta)^2] \tag{23}$$

and the energy spectrum from inertia subrange to maximum containing-energy eddy can be defined through the following Von-Karman function[24]

$$E_2(n) = 1.703\, u'^2 \lambda_{\mathrm{e}} (n\lambda_{\mathrm{e}})^4 / [1 + (n\lambda_{\mathrm{e}})^2]^{17/6} \tag{24}$$

where, λ_{e} denotes the mean size of containing-energy eddies, which has a major contribution to total turbulent kinetic energy. λ_{e} is usually obtained by measuring the Taylor micro-scale, λ_{T}.[28] The energy dissipation rate and λ_{T} have the following relationship[24]

$$\varepsilon = 15\nu u'^2 / \lambda_{\mathrm{T}}^2 = \beta_0 u'^3 / \lambda_{\mathrm{e}} \tag{25}$$

Thus, the relationship between λ_{e} and λ_{T} can be obtained

$$\lambda_{\mathrm{e}} = \beta_0 \lambda_T^3 \sqrt{\frac{\varepsilon}{(15\nu)^3}} \tag{26}$$

In addition, there are some reports on the experiential method in the literature, where λ_{e} is usually thought of as dependent on the device characteristic size of d (e.g., the diameter of stirred tank impeller or bubble column). Kresta et al. have listed a typical range, that is, $\lambda_{\mathrm{e}} = 0.08d$–$0.5d$.[29] McManamey et al. have shown that taking λ_{e} as $0.3d$ can approach to the experimental results for stirred tanks well.[30] As a matter of fact, λ_{e} is associated not only with reactor scale but also with turbulence intensity and varies with operation conditions. In the present study, we use the following formula to estimate λ_{e}

$$\varepsilon = \int_0^\infty 2\nu n^2 E(n) dn = 2\nu \int_{n_{\min}}^{n_{\max}} n^2 E(n) dn = f(\lambda_{\mathrm{e}}) \tag{27}$$

where ε is the average turbulent energy dissipation rate per unit mass fluid. In the literature, the methods for estimating ε may be different for various reactors such as bubble columns and stirred tanks,[10,31] nevertheless they are all based on the same principle, that is, the ratio of total input power to total fluid mass. The energy dissipation rate in Eq. 27 is usually a known condition and $2\nu \int_{n\min}^{n\max} n^2 E(n) dn$ is a function with respect to λ_{e}. Thus, λ_{e} can be estimated by Eq. 27 with a trial-error method. According to this method, we can take different values of λ_{e} from 0 to d (where d denotes the diameter of impeller or bubble column) and compare the dissipation rates calculated by Eq. 27 with the known value of dissipation rate, when the calculated and the known values are equal or the difference between them is less than a certain limit (e.g., 1×10^{-6}), the corresponding value of λ_{e} is the average size of containing-energy eddies.

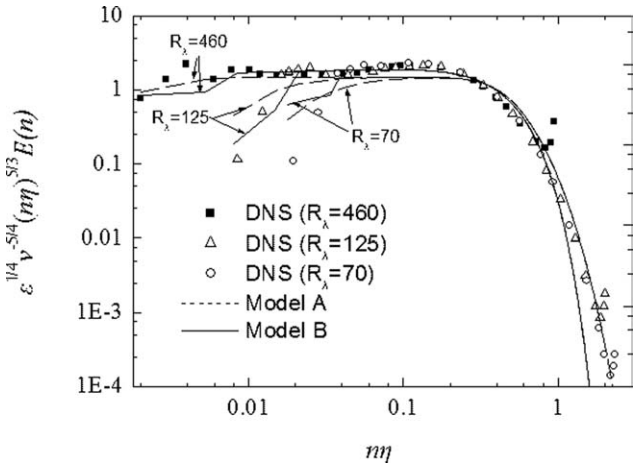

Figure 1. Comparison of the results calculated by full energy spectrum functions and the direct numerical simulation results.

Figure 1 depicts the difference between the results predicted by the two energy spectrum models above mentioned. It can be seen that in the energy-containing range and the dissipation range the results predicted by Model A show a better approach to that of direct numerical simulation (DNS),[32] the predicted upper border of inertia subrange also shows a good agreement with that of DNS. It should be noted that the precise three-dimensional energy spectrum is difficult to be obtained at present due to the fact that the turbulence structures have not yet been clarified completely.

Results and Discussion

Average mass transfer coefficient of single eddy, $\overline{k}_\lambda$

If considering steady-state mass transfer, $\overline{k}_\lambda$ can be calculated through the following simplified expression

$$\overline{k}_\lambda = C_n\sqrt{D}E(n)^{1/4}n^{3/2} \tag{28}$$

where $C_n = \frac{2\sqrt{2c_1}}{\pi}\int_0^{\pi/2}\sqrt{\cos(\varphi)}\,d\,\varphi \approx 0.682$. It can be seen from Figure 2 that with the increase of wave number (i.e., the decrease of eddy size), $\overline{k}_\lambda$ decreases in the dissipation range and increases in the other ranges. The inflexion locates on the upper border of inertia subrange. These curved lines shown in Figure 2 actually correspond to the non-monotonic relationship between energy spectrum and wave number (see Eq. 28). With the increase of wave number, turbulent eddy kinetic energy decreases sharply in the dissipation range (see Figure 1), this may lead to a decrease of $\overline{k}_\lambda$. Whereas in the other ranges, although turbulent eddy kinetic energy also decreases gradually with the increase of wave number, the number of eddies will increase rapidly due to the continual breakup of eddies, which may result in an increasing probability that eddies contact the surface, thus $\overline{k}_\lambda$ will also show an increasing trend. In addition, Figure 2 shows an increase of $\overline{k}_\lambda$ with increasing dissipation rate and $\overline{k}_\lambda$ in the dissipation range is larger than that in the other ranges.

Determination of depth of liquid film, δ

As mentioned before, in the film penetration or surface renewal models, the depth of liquid film was usually assumed to be infinite. This assumption can greatly simplify the problem, but may be not true (some investigators also made similar suggestions[4,5,8,10]). In a sense, the liquid film has an analogy to the boundary layer in turbulent flows and is very thin. Thus, the depth of liquid film may be a finite value. Nevertheless, there is no relevant comparison of the effect of the depth on the mass transfer coefficient in the literature. We will examine several different values of depth, that is, infinity, the size of current eddy contacting the surface, Kolmogorov scale η, and the sizes that are smaller than η. Then Eq. 19ii can be written as

(1) for the infinite depth ($\delta = \infty$)

$$k_{\mathrm{L}} = \frac{2\sqrt{2c_1D}}{\pi\int_{n_d}^{n_u}E(n)dn}\int_{n_d}^{\mathrm{n_u}}\int_0^{\pi/2}E(n)^{5/4}n^{3/4}\sqrt{\cos(\varphi)}d\varphi dn = \frac{\mathrm{C}_n\sqrt{\mathrm{D}}\int_{n_d}^{\mathrm{n_u}}E(n)^{5/4}n^{3/4}dn}{\int_{n_d}^{\mathrm{n_u}}E(n)dn} \tag{29}$$

where, the constant C_{n} is about 0.682.

(2) for the depth of current eddy size ($\delta = \lambda$)

$$k_{\mathrm{L}} = \frac{2\sqrt{2c_1D}}{\pi\int_{n_d}^{n_u}E(n)dn}\int_{n_d}^{\mathrm{n_u}}\int_0^{\pi/2}\times\frac{E(n)^{5/4}n^{3/4}\sqrt{\cos(\varphi)}}{\mathrm{erf}\left(\sqrt{c_1\pi/2D}E(n)^{1/4}n^{-1/4}\sqrt{\cos(\varphi)}\right)}d\varphi dn \tag{30}$$

(3) for the depth equal to or smaller than η ($\delta = p\eta = pv^3/\varepsilon$)

$$k_{\mathrm{L}} = \frac{2\sqrt{2c_1D}}{\pi\int_{n_d}^{n_u}E(\mathrm{n})dn}\int_{n_d}^{\mathrm{n_u}}\int_0^{\pi/2}\frac{E(n)^{5/4}n^{3/4}\sqrt{\cos(\varphi)}}{\mathrm{erf}\left(\sqrt{c_1\pi/2D}(\mathrm{p}/\varepsilon)^{-1/4}v^{3/4}E(n)^{1/4}n^{3/4}\sqrt{\cos(\varphi)}\right)}d\varphi d\mathrm{n} \tag{31}$$

where p is a constant. Here, four different values are taken as 1, 0.5, 0.3, and 0.1, respectively.

The experimental data of Fortescue and Pearson,[9] Bouaifi et al.,[14] and Davies and Lozano[33] shown in Figures 3–6 were used to test the proposed model at various turbulence levels (low

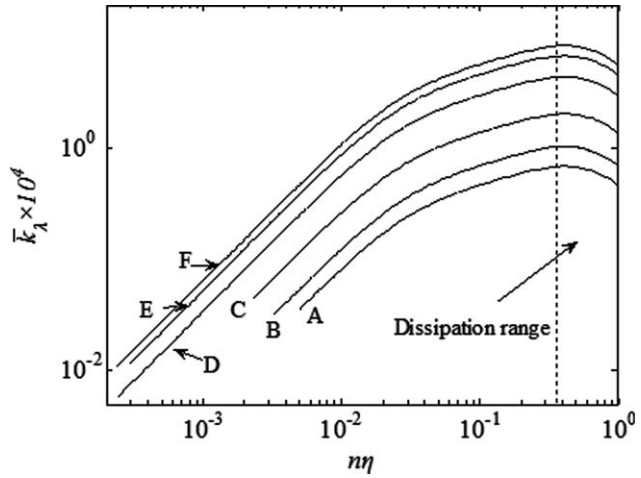

Figure 2. The predicted single-eddy mass transfer coefficient.

$\varepsilon \times 10^3$ m^2 s^{-3}: A—0.409, B—2.06, C—22.2, D—488.465, E—2760.761, F—6381.068.

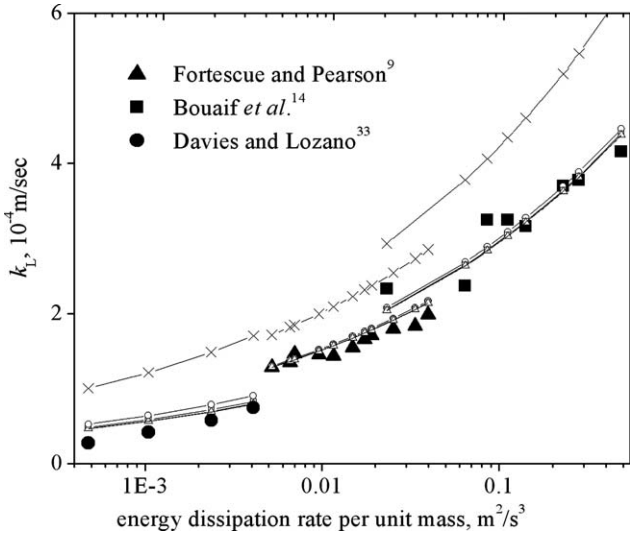

Figure 3. The effect of depth of liquid film on the average mass transfer coefficient.

—×—: 0.1η; —○—: 0.3η; —□—: 0.5η; —Δ—: η; ……: λ; — — —: ∞.

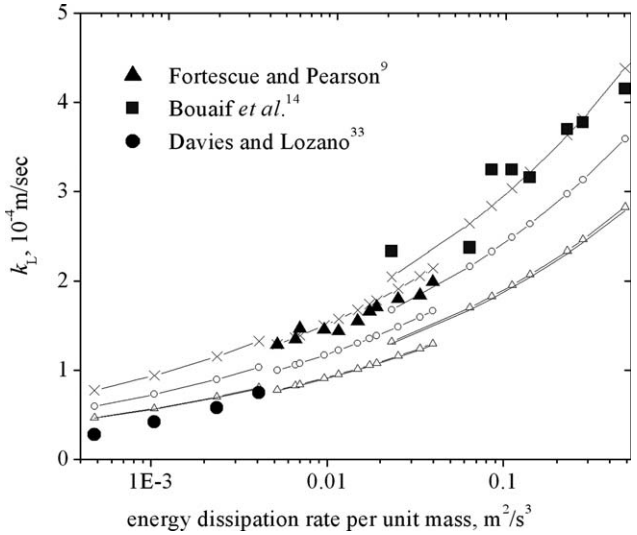

Figure 4. The effect of integration limit *n*d on the average mass transfer coefficient.

—×—: dissipation range; —○—: from η to λ_i;—Δ—: from η to λ_e; — — —: from η to d.

and high turbulent dissipation rates), where they measured the liquid-side mass transfer coefficient for CO_2-water[9] and O_2-water[14,33] systems at room temperature, the turbulence was generated by a duct of 0.038 m in deep where water flowed through grids in the Fortescue and Pearson's experiment, a vessel of diameter 0.43 m with dual axial flow impellers of diameter 0.143 m was used in the Boufai et al.'s experiment and a vessel of diameter 0.102 m with a flat bladed stirrer of diameter 0.0319 m was used by Davies et al. We note that the turbulent dissipation rates per unit mass needed for applying the present model were not given by Fortescue and Pearson,[9] which will be estimated through the relationship given by Lamont and Scott[10] for pipe flows: $\varepsilon \approx 0.16Re^{2.75}\upsilon^3/d^4$. The data of Davies and Lozano[33] at four low Reynolds numbers were adopted to test the present model at low turbulent dissipation rates where the dissipation rates were estimated through their measured turbulent intensities near free surface and integral lengths ($\varepsilon = \overline{u'^3}/\lambda_L$).

Figure 3 shows the predicted average mass transfer coefficient at different turbulent dissipation rates. It can be seen that the mass transfer coefficient predicted by the depth of 0.1η is obviously higher than those predicted by the other depths and is also much higher than the experimental data. When the depth exceeds 0.5η, increasing the depth will only have little effect on the average mass transfer coefficient. In particular, when taking the current eddy size and infinity as the depth, respectively, the predicted results are almost coincident. This is since the denominator in Eq. 19ii is an error function, with increasing z (let's define $z = \delta\sqrt{\boldsymbol{c_1}\pi/\boldsymbol{2D}\,\boldsymbol{E}(\boldsymbol{n})^{1/4}\boldsymbol{n}^{3/4}\sqrt{\cos(\varphi)}}$), the function value tends to one quickly (e.g., when $z \geq 2.0$, erf $(z) \approx 1$), so even though taking the considerable depth, the predicted results are hardly influenced, but when taking very small depth, for example 0.1η or 0.3η, the variable z may become much smaller than 2, the values of depth will evidently influence the average mass transfer coefficient.

Here, taking the size of current eddy contacting the surface as the depth appears to more approach to the actual situation, because the depth of liquid film may not be a fixed value and depend on eddy size. It should be noted that in the process of nearing the surface, the eddy is usually deformed and stretched continually, and forms a complex shape, the precise depth is difficult to be determined. Although the assumption of infinity is inconsistent with many actual situations, it may be acceptable for the sake of convenience.[8]

Determination of integration limit, $\mathbf{n}_d$

In the literature, there are mainly two concepts, which were used to describe the fluid in liquid side of surface, that

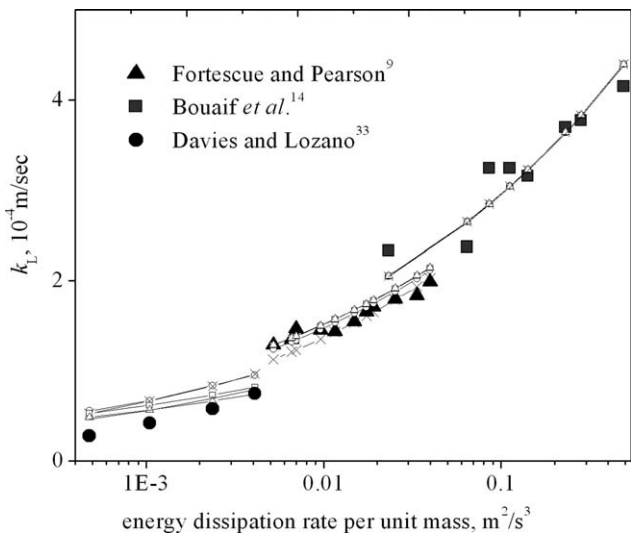

Figure 5. The effect of average containing-energy eddy size on the average mass transfer coefficient.

—×—: $\lambda_e = 0.05d$; —○—: $\lambda_e = 0.1d$; —□—: $\lambda_e = 0.3d$; —Δ—: $\lambda_e = 0.5d$; — — —: estimated by Eq. 27.

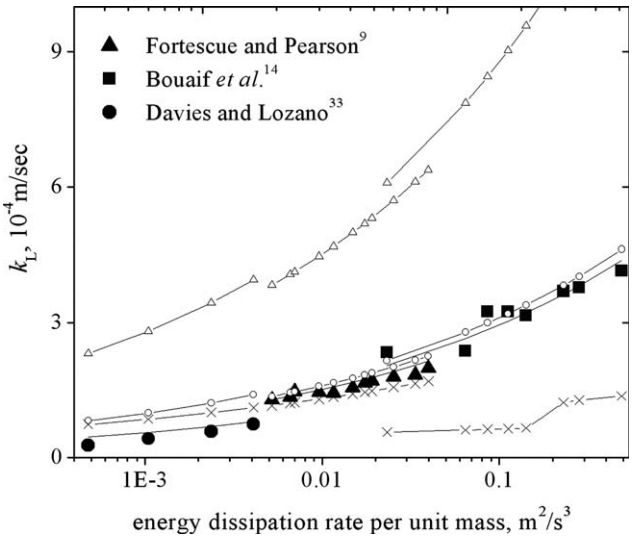

Figure 6. The effect of energy spectrum function on the average mass transfer coefficient.

—Δ—: $c0$ = 1.13 (Kawase et al.[19]); —○—: $c0$ = 0.4 (Lamout et al.[10]); —×—: Model B; — — —: Model A.

is, "fluid element" and "eddy." They are usually regarded as the same concept and above discussions also don't differentiate them. Here, it is worth noting that the "fluid element" seems abstract, its size is uncertain and more importantly, it is not easy to associate fluid element with turbulence micro-structure parameters such as ε, while adopting the "eddy" is convenient for us to understand mass transfer process and apply the turbulence theory. Thereby, "eddy" is more recommendable in the case of turbulent flows, whereas it appears unsuitable for the quiescent fluid or laminar flows.

Several models based on the eddy concept have been presented in the literature, as mentioned above, most of them assumed that mass transfer process is mainly controlled by a certain range of eddies before developing the relevant model, for example the large-eddy model and the small-eddy model. In fact, all eddies might have contributions to the mass transfer process, but the issue of controlling factor may exist. Such contributions are associated with turbulence intensity and surface property in nature, purely presupposing that the process is controlled by a certain range of eddies may be one-sided. In the present study, to account for the effect of eddies with different sizes on the average mass transfer coefficient, we examine several upper limit values for n_d appearing in Eq. 19ii, that is, the characterize size of reactor d (the diameter of stirred tank impeller or bubble column), the average containing-energy eddy size λ_e, $\lambda_e/6$ (at high R_λ, it equals λ_i, which is the upper border of inertia subrange approximately) and the upper border of dissipation range, they will be transformed into corresponding wave numbers before solving Eq. 19ii.

Figure 4 shows the effect of upper limit value for n_d on the average mass transfer coefficient. It can be seen that at low turbulence intensities (i.e., ε is less than about 0.005 m^2 s^{-3}), when taking λ_e as the upper limit, the predicted results are satisfactory in comparison with the reported experimental data, taking the upper limit as a value larger than λ_e (e.g., d) has little effect on the results, whereas when taking the upper limit as a value smaller than λ_e (e.g., $\lambda_e/6$ or the upper border of dissipation range), the average mass transfer coefficient will be overestimated. At higher turbulence intensities (over about 0.005 m^2 s^{-3}), a good agreement can be obtained in comparison with the experimental data when taking the upper border of dissipation range as n_d, while the results will be underestimated with the increasing n_d.

The effect of n_d on the mass transfer coefficient shown in Figure 4 can be explained by the contributions of eddies with different sizes to mass transfer process. In turbulent flows, the number of eddies of size larger than the average containing-energy eddy is usually much smaller than that of the other eddies, this means that the chance of these eddies contacting the surface will reduce obviously and their overall contribution to mass transfer is limited. Thus, the results predicted by the limit of d show an approach to that by the limit of λ_e. On the other hand, at low turbulence intensities, the breadth of the eddies size distribution existing in turbulent flow field is smaller than that at high turbulence intensities and the inertia subrange is very narrow and even absent. Thus the dissipation range and the energy containing range may be linked up and even be overlapped partly, the contribution of eddies in the energy containing range to mass transfer may become important. However in the case of high turbulence intensities, there is a clear inertia subrange and the number of eddies may increase obviously in the dissipation range due to higher dissipation rate and smaller size of the smallest viscosity eddy (viz. Kolmogorov scale). These eddies in the dissipation range may govern mass transfer process. It should be noted that the proportion coefficient c_1 (=0.4) in Eq. 17 given by Lamont and Scott is based on the isotropic turbulence theory. Strictly speaking, it is not suitable for the whole energy containing range since anisotropy will become stronger with the increase of eddy size. If the energy spectrum function and the velocity amplitude in the whole energy containing range can be obtained accurately, this limitation will no longer exist.

Table 1. The Estimated Average Containing-Energy Eddy Size, λ_e

Bubble Column (CO_2-water, d = 0.045 m)		Stirred Tank (Air–Water, d = 0.0319 m)		Stirred Tank (Air–Water, d = 0.075 m)	
$\varepsilon \times 10^3$(m^2 s^{-3})	λ_e/d (–)	$\varepsilon \times 10^3$(m^2 s^{-3})	λ_e/d (–)	$\varepsilon \times 10^3$(m^2 s^{-3})	λ_e/d (–)
0.409	0.4542	0.59	0.5850	27.687	0.0950
0.675	0.4008	1.42	0.4695	211.029	0.0572
1.030	0.3606	4.81	0.3462	1485.575	0.0351
1.490	0.3288	7.61	0.3086	3176.011	0.0290
2.750	0.2821	16.2	0.2554	6381.067	0.0244

Determination of average containing-energy eddy size, λ_e

Table 1 shows the calculated λ_e through Eqs. 21 and 27. It can be seen that the assumption of uniform size (e.g., $0.3d$ or $0.5d$) is too simple and actually λ_e decreases with increasing dissipation rate. Figure 5 gives the comparison of average mass transfer coefficients predicted by different values of λ_e. It can be seen that the predicted results decrease with increasing λ_e. In turbulent flows, the frequent breakup of eddies has an important effect on λ_e until it is prevented by viscous effect and the smallest viscosity eddy is formed, it may be the main reason that λ_e varies with ε.

For the relationship between λ_e and ε, there is no theoretical model available in the literature. λ_e is usually determined experimentally. Here, λ_e is estimated by Eqs. 21 and 27, the estimated results are encouraging since they show a good agreement with the experimental data (as shown in Figure 5). It should be noted that the influence of λ_e on the mass transfer coefficient is not obvious at high turbulence intensities (ε is larger than 0.02 m^2 s^{-3}). This is because the upper border of dissipation range is taken as the upper integration limit and the energy spectrum function is nearly independent on λ_e in the dissipation range (let's define $f_L = \left(n\lambda_e / \left[(n\lambda_e)^2 + c_L\right]^{1/2}\right)^{5/3+p_0}$, it goes to one for large wave number, see Eq. 21). This means that only assigning a fixed value such as $0.3d$ or $0.5d$ can also give a satisfactory result, this feature makes the present model more convenient to be applied for highly turbulent flows.

Determination of energy spectrum function, E(n)

When using Model A, the average mass transfer coefficient is predicted by Eq. 19, while using Model B, the average mass transfer coefficient is predicted by the following formula

$$k_L = \frac{\int_{n_i}^{n_u} \overline{k}_\lambda E_2(n)dn + \int_{n_d}^{n_i} \overline{k}_\lambda E_1(n)dn}{\int_{n_i}^{n_u} E_2(n)dn + \int_{n_d}^{n_i} E_1(n)dn} = C_n\sqrt{D}\,\frac{\int_{n_i}^{n_u} E_2(n)^{5/4}n^{3/4}dn + \int_{n_d}^{n_i} E_1(n)^{5/4}n^{3/4}dn}{\int_{n_i}^{n_u} E_2(n)dn + \int_{n_d}^{n_i} E_1(n)dn} \quad (32)$$

Where, n_i is the upper border of inertia subrange, which is usually evaluated by making $E_1(n) = E_2(n)$. It is not difficult to find that at high R_λ, n_i evaluated by this method can lie only in the dissipation range and not on the real upper border of inertia subrange (see Figure 1). This means that the energy spectrum function in the inertia subrange, which should have been used, may be substituted by that in the energy containing range. Thereby, it will cause some errors at high turbulence intensities. Whereas the method of combining Model A (i.e., Eq. 21) with Eq. 19 doesn't need to evaluate n_i and the results predicted by this method show a better agreement with the experimental data (shown in Figure 6).

In addition, Figure 6 gives the results predicted by the two models often mentioned in the literature, *viz.* the penetration model with $c_0 = 1.13$[19] and the eddy cell model with $c_0 = 0.4$.[10] It can be seen that the penetration model obviously overestimates the average mass transfer coefficient whether at low or at high turbulence intensities and the eddy cell model can give good results only at high turbulence intensities (which fairly approach to those predicted by the method of combining Model A with Eq. 19), but at low turbulence intensities the eddy cell model also overestimates the results obviously. Figure 6 shows that the method of combining Model A with Eq. 19 can give a good agreement with the experimental data in a considerably wide range of turbulence intensities.

Discussion of contact time, τ_e

From the comparison of the predicted results and experimental data shown in Figures 3–6, it indicates that the steady-state mass transfer mechanism for single eddy (i.e., Eq. 19ii) is fairly acceptable since the predicted results are satisfying. Nevertheless, it may be valuable to discuss the unsteady-state mass transfer through Eq. 19i. We note that the interaction between eddy and bubble surface was usually assumed to be a rigid collision in the most existing models for bubble breakup, this means that this interaction is instantaneous. The assumption seems contradictory to the classical mass transfer theory because an instantaneous interaction means that contact time tends to zero, then mass transfer coefficient will tend to infinity according to the penetration or surface renewal theory. This is inconsistent with the experimental results. Therefore, there is a specific time for the contact process but the contact time distribution at the surface may not be uniform but obey a random bounded by certain parameters such as eddy size, turbulent eddy kinetic energy and viscosity. In the literature, there are two typical models for evaluating this time, viz. the "eddy" models, which used the characteristic time of the smallest viscosity eddy (Kolmogorov time scale) as the contact time and the "slip penetration" model, which used the ratio of bubble diameter to slip velocity as the contact time. The two models have been supported only by some experimental data in a certain limited range of turbulence intensities, the reason may be illustrated by the details of contact process.

During the contact process or just at the moment of mother eddies arriving at bubble surface, some fresh daughter eddies may be generated due to the breakup of mother eddies, in addition, some eddies may keep contacting with bubble surface until they die out or are pushed out by following eddies. In these cases, the "eddy" models are not applicable since the actual contact time is usually not equal to the characteristic time of the smallest viscosity eddy, the "slip penetration" model also seems unsuitable for the highly turbulent flows since eddies contact bubble surface frequently at high fluctuation velocity and thus bubble surface will be deformed with a complex shape and may break up eventually, this leads to that bubble diameter varies with time. Experimental observations have shown that the average deformation degree that results in breakup may reach 2–3 d_0.[34] Therefore, using the initial or a fixed bubble diameter is not suitable for highly turbulent flow. It may be one of the main reasons that the experimental data don't support the "slip penetration" model. If using the bubble diameter varying with time, it is possible to improve the prediction.

To account for the effect of contact time on the average mass transfer coefficient, we try to test several specific

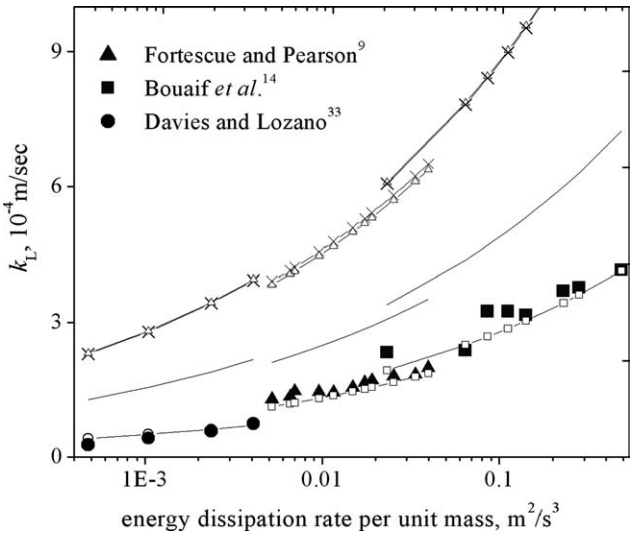

Figure 7. The effect of contact time on the average mass transfer coefficient.

—Δ—: $c0 = 1.13$ (Kawase et al.[19]); —×—: Kolmogorov time scale; —□—: two time scales with scaling factor 0.532; — — —: two time scales; —○—: two time scales with scaling factor 0.328.

values through defining the following two time scales. In the dissipation range, contact time is

$$\tau_e = (v/\varepsilon)^{1/2}. \tag{33}$$

and in the other ranges, contact time is

$$\tau_e = (\lambda^2/\varepsilon)^{1/3} \tag{34}$$

Figure 7 shows the average mass transfer coefficient predicted by several methods, where the whole range of energy spectrum (i.e., from η to d) is considered. It can be seen that the method of two time scales can give obviously lower results than those given by the method of only using Kolmogorov time scale (i.e., Eq. 33), but both the methods overestimate the averaged mass transfer coefficient. It may need to make the time scale higher to obtain lower mass transfer coefficients, but according to the turbulence theory, the contact time of an eddy cannot be longer than the characteristic time of the eddy. One of the possible reasons is that the uniform distribution of contact time and the direct proportion relationship between contact time and eddy size (see Eq. 34) are too rough to be correct and the real time distribution at the surface is very complicated. Figure 7 also implies that the premise of obtaining ideal predicted results for the unsteady-state model is to estimate the contact time distribution properly.

It can be seen from Figure 7, the predicted results by the method of two time scales that are modified by a scaling factor show a very good agreement with the experimental data. However, when turbulence intensity varies, the scaling factor also needs to be adjusted accordingly. This method is similar to a semi-empirical correlation and thus cannot be extended. In Figure 7, it also shows that if using the uniform Kolmogorov time scale, the results predicted by Eq. 19i almost coincide with those by the penetration model with $c_0 = 1.13$.[19]

An alternative and effective approach is using the steady-state model (i.e., combining Eq. 19ii with Model A) , which can avoid the problem of determining the contact time and is more convenient to be applied.

The average deviation of the average mass transfer coefficient

The available experimental data on gas–liquid mass transfer coefficient k_L are limited in the literature and most results are the volumetric coefficient k_La, where a is the specific interfacial area, which can be calculated from gas holdup and bubble size distribution. The traditional method for estimating a is based on semi-theoretic correlations. Several equations based on this method for different systems can be found in the literature.[35–37] In recent years, many investigators[38–43] have devoted their efforts to the method of population balance model (PBM). The gas holdup and the bubble size distribution can be predicted by CFD coupled with PBM.[44–46] It should be noted that there is an accumulative error resulting from the product of the two estimated errors of k_L and a, and the global parameter of k_La may be insufficient for judging the capability of mass transfer coefficient models and understanding the mass transfer mechanism. Therefore, it is necessary to separate k_L from k_La and put emphasis on k_L.[14,37,46,47]

Figure 8 shows the comparison of the predicted k_L and the available experimental data. It can be seen that the average deviation (which is defined as: (calculated value−experimental value)/experimental value) is only about ±10%, it is in satisfactory agreement at a wide range of turbulence intensities. The Linke et al.'s data for oxygen-water system shown in Figure 8 were obtained from the experiments performed in a flat-bottomed cylindrical vessel with internal diameter 0.19 m equipped with a standard Rushton turbine of 0.075 m in diameter,[15] where the mean turbulent dissipation rate varied from about 0.02 $m^2\ s^{-3}$ to 6.4 $m^2\ s^{-3}$. All the values of $k_{L,calc}$ shown in Figure 8 are calculated from the steady-state model

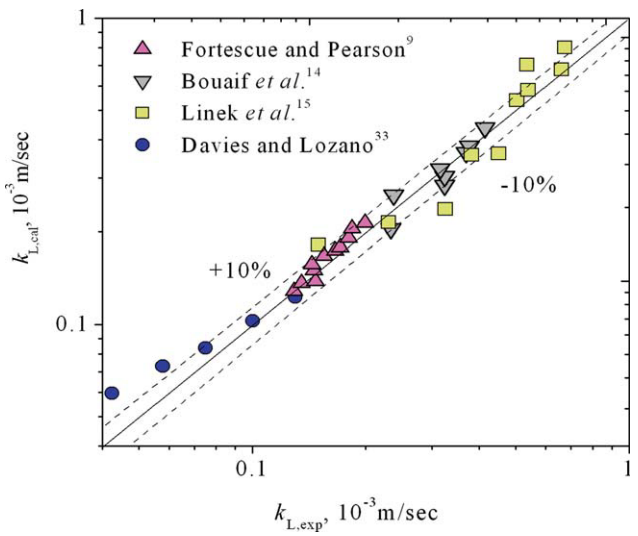

Figure 8. The comparison of predicted *k*L and the available experimental data.

[Color figure can be viewed in the online issue, which is available at wileyonlinelibrary.com.]

(Eq. 19ii), where the wave spectrum from η to d is used for ε being less than about 0.005 $m^2\ s^{-3}$ and the wave spectrum in the dissipation range is used for ε being more than about 0.005 $m^2\ s^{-3}$. In addition, the required energy spectrum $E(n)$ is calculated from Model A and the containing energy eddy scale λ_e is estimated by Eq. 27.

Conclusions

A multi-scale theoretical model (Eq. 19) based on the wide spectrum eddy contact concept and the isotropic turbulence theory has been developed successfully for the determination of the gas–liquid interface mass transfer coefficient from an unsteady-state convection and diffusion mechanism. This model has considered the contributions of eddies with different sizes in a wide range of wave spectrum to the overall mass transfer coefficient and can be regarded as a general mass transfer model since the predicted results by the unsteady-state model (Eq. 19i) show a coincidence with those by the penetration model with $c_0 = 1.13$[19] when taking Kolmogorov time scale as the contact time and the steady-state model (Eq. 19ii) also gives very similar results to the eddy cell model with $c_0 = 0.4$[10] when only considering the dissipation range.

The unsteady-state mass transfer mechanism seems not easy to be applied due to that the true contact time distribution on the surface is very complicated and difficult to be determined. Several values of contact time were tested, the results predicted by the method of scaling factor show a very good agreement with the experimental data, nevertheless which usually can't be extended. With no scaling factor, the unsteady-state model overestimated the results. An effective approach of avoiding the determination of contact time is to assume a steady-state mass transfer mechanism for single eddy. This mechanism is fairly acceptable since the predicted results are in good agreement with the experimental data in a comparatively wide range of turbulence intensities. Moreover, the steady state model is not sensitive for the values of δ, except that it is much smaller than Kolmogorov scale. The results by the depth of current eddy size fairly approach to those by the depth of infinity, it may be regarded as the sake of supporting the use of infinite depth.

Acknowledgments

The authors acknowledge the financial support from the National Natural Science Foundation of China (No. 20776121) and the Scientific Fund of Hunan Provincial Education Department (No. 07C765).

Notation

a = specific interfacial area, $m^2\ m^{-3}$
A = velocity amplitude, $m\ s^{-1}$
c_b, c_s = the bulk and surface concentration of species, respectively, $mol\ m^{-3}$
c_0,c = proportion coefficient of model
C_1,C_2,C_n = constant
d_0 = initial diameter of the bubble, m
d = diameter of impeller, m
D = molecular diffusivity, $m^2\ s^{-1}$
$E(n)$ = energy spectrum function
k_L = mass transfer coefficient, $m\ s^{-1}$
K_T = power number
M = total liquid mass, kg
n = wave number, m^{-1}
n_u, n_d, n_{max}, n_{min} = integration limit, m^{-1}
P = power, W
R_λ = Taylor-scale Reynolds number
t = time, s
u = velocity, $m\ s^{-1}$
u' = fluctuation velocity, $m\ s^{-1}$
v = velocity, $m\ s^{-1}$
x = coordinate parallel to the surface
y = coordinate perpendicular to the surface
β_0 = constant
δ = depth of liquid film, m
ε = turbulent energy dissipation of per unit mass, $m^2\ s^{-3}$
η = Kolmogorov scale, m
λ = length scale of eddy, m
λ_e = average size of containing-energy eddies, m
λ_i = upper border of inertia subrange, m
λ_L = integral length, m
λ_T = Taylor micro-scale, m
ρ = liquid density, $kg\ m^{-3}$
τ_e = exposure (or contact) time, s
υ = kinematic viscosity, $m^2\ s^{-1}$

Literature Cited

1. Lewis WK, Whitman WG. Principles of gas absorption. *Ind Eng Chem*. 1924;16:1215–1220.
2. Higbie R. The rate of absorption of a pure gas into a still liquid during short periods of exposure. *Trans Am Inst Chem Eng*. 1935;31:365–389.
3. Danckwerts PV. Significance of liquid–film coefficients in gas absorption. *Ind Eng Chem*. 1951;43:1460–1467.
4. Dobbins WE. *The Nature of the Oxygen Transfer Coefficient in Aeration Systems. Biological Treatment of Sewage and Industrial Wastes*, pt. 2–1. New York: Reinhold, 1956;1:141–148.
5. Toor HL, Marchello JM. Film-penetration model for mass and heat transfer. *AIChE J*. 1958;4:97–101.
6. Angelo JB, Lightfoot EN, Howard DW. Generalization of the penetration theory for surface stretch: application to forming and oscillation drops. *AIChE J*. 1966;12:751–760.
7. Stewart WE, Angelo JB, Lightfoot EN. Forced convection in three-dimensional flows: II. *AIChE J*. 1970;16:771–786.
8. Jajuee B, Margaritis A, Karamanev D, Bergougnou MA. Application of surface-renewal -stretch model for interface mass transfer. *Chem Eng Sci*. 2006;61:3917–3929.
9. Fortescue GE, Pearson JRA. On gas absorption into a turbulent liquid. *Chem Eng Sci*. 1967;22:1163–1176.
10. Lamont JC, Scott DS. An eddy cell model of mass transfer into the surface of a turbulent liquid. *AIChE J*. 1970;16:513–519.
11. Luk S, Lee YH. Mass transfer in eddies close to air-water interface. *AIChE J*. 1986;32:1546–1554.
12. Luo HA, Hu RR, Liu PL, Wang LJ. Eddy model for gas–liquid mass transfer coefficient at free surface. *J Chem Ind Eng (China)*. 2002;53:1164–1168.
13. Petty CA. A statistical theory for mass transfer near interfaces. *Chem Eng Sci*. 1975;30:413–418.
14. Bouaifi M, Hebrard G, Bastoul D, Roustan M. A comparative study of gas hold-up, bubble size, interfacial area and mass transfer coefficients in stirred gas–liquid reactors and bubble columns. *Chem Eng Proc*. 2001;40:97–111.
15. Linek V, Kordač M, Moucha T. Mechanism of mass transfer from bubbles in dispersions Part II: mass transfer coefficients in stirred gas–liquid reactor and bubble column. *Chem Eng Proc*. 2005;44:121–130.
16. Hu LS, Wang XJ, Yu GS, Wang FC, Yu ZH. Study on gas–liquid phase mass transfer coefficient of entrained flow reactor. *Chem Eng J*. 2008;141:278–283.
17. Kawase Y, Halard B, Moo-Young M. Liquid-phase mass transfer coefficients in bioreactors. *Biotechnol Bioeng*. 1992;39:1133–1140.
18. Prasher BD, Wills GB. Mass transfer in an agitated vessel. *IEC Proc Des Dev*. 1973;12:351–354.

19. Kawase Y, Halard B, Moo-Young M. Theoretical prediction of volumetric mass transfer coefficients in bubble columns for Newtonian and non-Newtonian fluids. *Chem Eng Sci*. 1987;42:1609–1617.
20. Alves SS, Vasconcelos JMT, Orvalho SP. Mass transfer to clean bubbles at low turbulent energy dissipation. *Chem Eng Sci*. 2006;61:1334–1337.
21. Davies JT, Lozano FJ. Turbulence and surface renewal at the clean surface of a stirred vessel. *AIChE J*. 1984;30:502–504.
22. Komori S, Murakami Y. Turbulent mixing in baffled stirred tanks with vertical-blade impellers. *AIChE J*. 1988;34:932–937.
23. Komori S, Nagaosa R, Murakami Y. Mass transfer into a turbulent liquid across the zero-shear gas–liquid interface. *AIChE J*. 1990;36:957–960.
24. Hinze JO. *Turbulence*. New York: McGraw-Hill, 1975.
25. Luo H, Svendsen HF. Theoretical model for drop and bubble breakup in turbulent dispersions, *AIChE J*. 1996;42:1225–1233.
26. Pope SB. *Turbulent Flows*. Cambridge: Cambridge University Press, 2000.
27. Yeung PK, Zhou Y. Universality of the Kolmogorov constants in numerical simulations of turbulence. *Phys Rev E*. 1997;56:1746.
28. Liepmann HW, Robinson MS. Counting Methods and Equipment for Mean-Value Measurements in Turbulence Research. Washington, DC: National Advisory Committee for Aeronautics. Technical Report No. 3037, 1953.
29. Kresta SM, Wood PE. The flow field produced by a pitched blade turbine: characterization of the turbulence and estimation of the dissipation rate. *Chem Eng Sci*. 1993;48:1761–1774.
30. McManamey WJ, Davies JT. Woollen JM, Coe JR. The influence of molecular diffusion on mass transfer between turbulent liquids. *Chem Eng Sci*. 1973;28:1061–1069.
31. Wang TF, Wang JF, Jin Y. Theoretical prediction of flow regime transition in bubble columns by the population balance mode. *Chem Eng Sci*. 2005;60:6199–6209.
32. Gotoh T, Fukuyama D, Nakano T. Velocity field statistics in homogeneous steady turbulence obtained using a high-resolution direct numerical simulation. *Phys Fluids*. 2002;14:1065.
33. Davies JT, Lozano FJ. Turbulence characteristics and mass transfer at air-water surfaces. *AIChE J*. 1979;25:405–415.
34. Andersson R, Andersson B. On the breakup of fluid particles in turbulent flows. *AIChE J*. 2006;52:2031–2038.
35. Joshi JB, Pandit AB, Sharma MM. Mechanically agitated gas–liquid reactors. *Chem Eng Sci*. 1982;37:813–844.
36. Barigou M, Greaves M. Gas holdup and interfacial area distributions in a mechanically agitated gas–liquid contactor. *Trans Inst Chem Eng*. 1996;74:397–405.
37. Garcia-Ochoa F, Gomez E. Theoretical prediction of gas–liquid mass transfer coefficient, specific area and holdup in sparged stirred tanks. *Chem Eng Sci*. 2004;59:2489–2501.
38. Millies M, Mewes D. Interfacial area density in bubbly flow. *Chem Eng Proc*. 1999;38:307–319.
39. Colella D, Vinci D, Bagatin R, Masi M, Bakr EA. A study on coalescence and breakage mechanisms in three different bubble columns. *Chem Eng Sci*. 1999;54:4767–4777.
40. Lehr F, Millies M, Mewes D. Bubble-size distributions and flow fields in bubble columns. *AIChE J*. 2002;48:2426–2443.
41. Ramkrishna D, Mahoney AW. Population balance modeling. Promise for the future. *Chem Eng Sci*. 2002;57:595–606.
42. Chen P, Sanyal J, Dudukovic MP. Numerical simulation of bubble columns flows: effect of different breakup and coalescence closures. *Chem Eng Sci*. 2005;60:1085–1101.
43. Wang TF, Wang JF, Jin Y. A CFD–PBM coupled model for gas–liquid flows. *AIChE J*. 2006;52:125–140.
44. Burris VL, McGinnis DF, Little JC. Predicting oxygen transfer and water flow rate in airlift aerators. *Water Res*. 2002;36:4605–4615.
45. Dhanasekharan KM, Sanyal J, Jain A, Haidari A. A generalized approach to model oxygen transfer in bioreactors using population balances and computational fluid dynamics. *Chem Eng Sci*. 2005;60:213–218.
46. Wang TF, Wang JF. Numerical simulations of gas–liquid mass transfer in bubble columns with a CFD–PBM coupled model. *Chem Eng Sci*. 2007;62:7107–7118.
47. Yang WG, Wang JF, Wang TF, Jin Y. Experimental study on gas–liquid interfacial area and mass transfer coefficient in three-phase circulating fluidized beds. *Chem Eng J*. 2001;84:485–490.

Manuscript received Mar. 30, 2009, revision received Mar. 18, 2010, and final revision received Jun. 4, 2010.